Bioconjugate Chemistry

Article

pubs.acs.org/bc

Rapid ^{18}F-Labeling and Loading of PEGylated Gold Nanoparticles for in Vivo Applications

Jun Zhu,[†,‡,§] Joshua Chin,[†,‡] Carmen Wängler,[∥] Bjoern Wängler,[⊥] R. Bruce Lennox,*[,‡] and Ralf Schirrmacher*[,†,§]

[†]Montreal Neurological Institute & Hospital, McGill University, 3801 University Street, Montreal, Quebec H3A 2B4, Canada

[‡]Department of Chemistry, McGill University and Centre for Self-Assembled Chemical Structures, 801 Sherbrooke St. West, Montreal, Quebec H3A 2K6, Canada

[§]Lady Davis Institute for Medical Research, Jewish General Hospital, McGill University, 3755 Côte Ste-Catherine Road, Montreal, Quebec H3T 1E2, Canada

[∥]Biomedical Chemistry, Department of Clinical Radiology and Nuclear Medicine and [⊥]Molecular Imaging and Radiopharmaceutical Chemistry, Department of Clinical Radiology and Nuclear Medicine, Medical Faculty Mannheim of Heidelberg University, 68167 Mannheim, Germany

Supporting Information

ABSTRACT: Water-soluble 3 nm maleimide-terminated PEGylated gold nanoparticles (maleimide-AuNP) were synthesized in both partially hydrolyzed and nonhydrolyzed forms. Both of these maleimide-AuNPs, when reacted with the silicon−fluorine prosthetic group [^{18}F]SiFA-SH, resulted in radiolabeled AuNPs. These NPs were readily purified with high radiochemical yields (RCY) of 60−80% via size exclusion chromatography. Preliminary small animal positron emission tomography (PET) measurements in healthy rats gives information about the pathway of excretion and the stability of the radioactive label in vivo. The partially hydrolyzed [^{18}F]SiFA-maleimide-AuNPs shows uptake in the brain region of interest (ROI) (> 0.13%ID/g) which was confirmed by ex vivo examination of the thoroughly perfused rat brain. The multiple maleimide end groups on the AuNP surface also allows for the simultaneous incorporation of [^{18}F]SiFA-SH and a bioactive peptide (cysteine-modified octreotate, cys-TATE, which can bind to somatostatin receptor subtypes 2 and 5) in a proof-of-concept study. The well-defined Michael addition reaction between various thiol containing molecules and the multifunctionalized maleimide-AuNPs thus offers an opportunity to develop a new bioconjugation platform for new diagnostics as well as therapeutics.

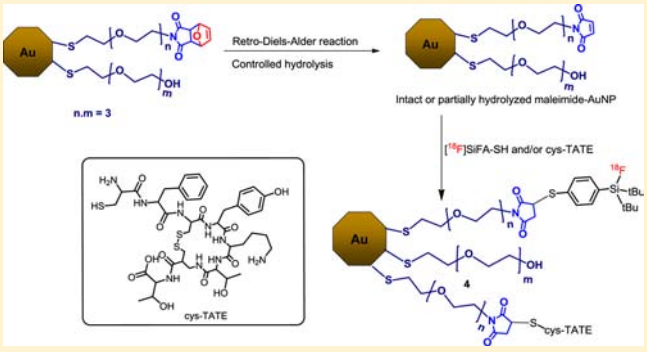

INTRODUCTION

Interest in the application of nanoparticles for in vivo diagnostic and therapeutic purposes has grown during the past decade as a result of their potential in early detection, accurate diagnostics, and even personalized treatment of various diseases.[1−3] Nanoparticles such as quantum dots, iron oxide nanoparticles, polymer nanoparticles, carbon nanotubes, and lipid nanoparticles have been used for the development of diagnostic probes and/or drug carriers in biomedical research.[1] Gold nanoparticles (AuNP) are among the most promising candidates for drug delivery due to the intrinsically low toxicity of the gold core, the potential for biocompatibility via functionalization, and their availability in a range of sizes and shapes. Most importantly, thiol-protected AuNPs display excellent stability and can be used in some selected chemical derivatization procedures, thus providing for postsynthesis modification aimed at improving their delivery efficiency and prolonging their circulation in the blood by reducing nonspecific organ uptake.[4−7] The potential to mediate the transfer of a molecule across the blood brain barrier (BBB) makes AuNPs an important development platform for brain research.[8]

Previous research by De Jong et al. has demonstrated that the tissue distribution of AuNPs is size dependent; the smallest (10 nm) AuNP in their study demonstrated widespread organ distribution.[9] Kreyling et al. confirmed a uniform distribution of AuNPs (11−31 nm, hydrodynamic size) in different organs.[10] Neither study reports detectable crossing of the BBB for AuNP >10 nm.[9,10] We have introduced a 3.2 ± 0.5 nm, water-soluble gold NP template that is functionalized with click chemistry-amenable maleimide derivatives.[10] Each gold core contains ca. 1000 gold atoms and is surrounded by ca. 30 furan protected

Received: April 11, 2014
Revised: May 7, 2014
Published: May 7, 2014

Scheme 1. Reaction Scheme of the Preparation of Maleimide-AuNPs (4, 7) and the Michael Addition Reaction of (4, 7) with ^{18}F Labeled SiFA-SH ([^{18}F]5) and/or Cysteine Derivative cys-TATE (9) Peptide[a]

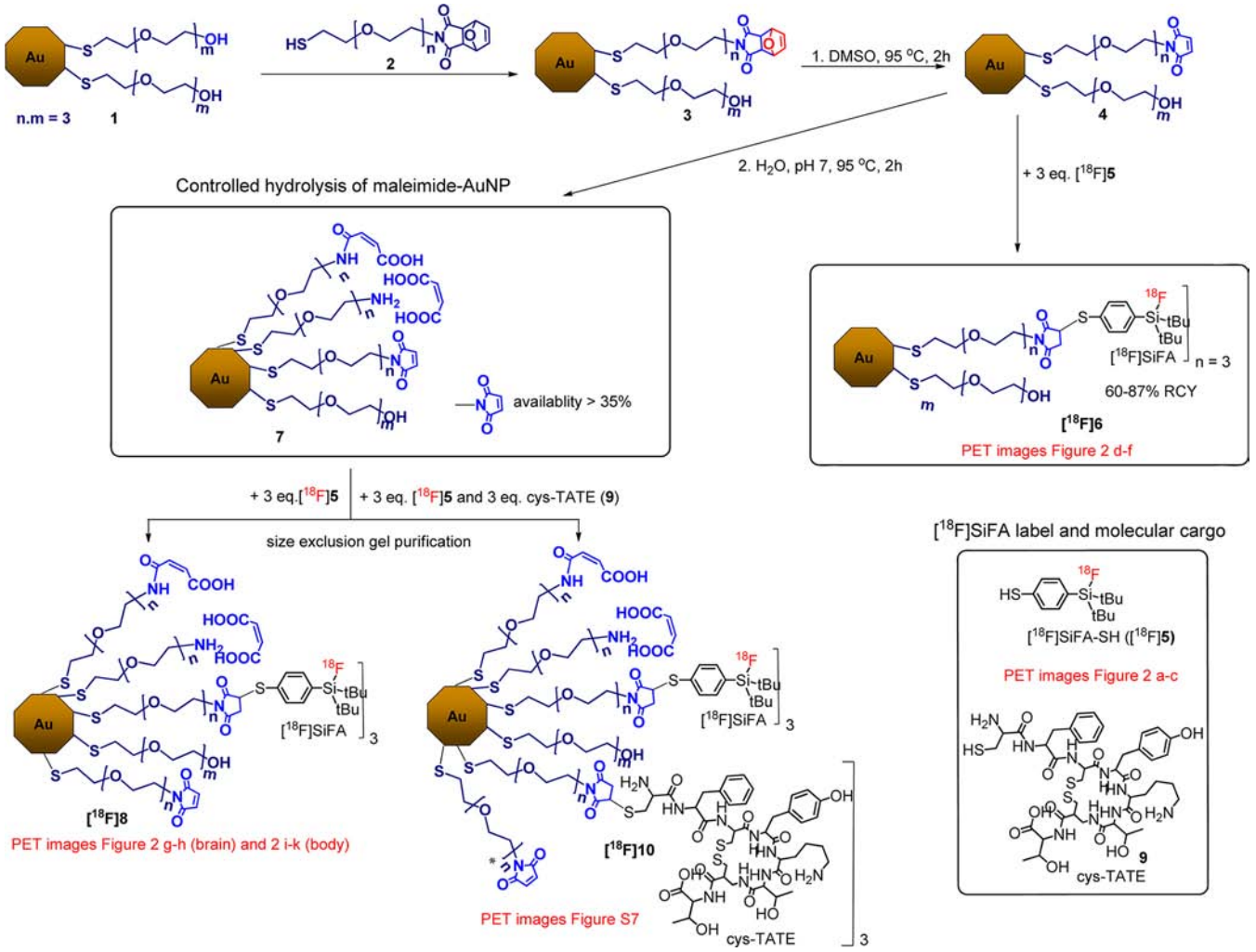

[a]The maleimide-AuNP (**4**) was first labeled with [^{18}F]**5** to generate [^{18}F]AuNP ([^{18}F]**6**) for PET studies. Deprotection of the furan protected maleimide-AuNP (**3**) in water-containing media resulted in hydrolysis of the maleimide moieties. A controlled hydrolysis of maleimide-AuNP (**4**) was carried out by heating **4** in water containing media for 2 h to generate partially hydrolyzed maleimide-AuNP (**7**) which then reacted with [^{18}F]**5** and/or 9 to give AuNPs [^{18}F]**8** and [^{18}F]**10** for micro PET evaluation.

maleimide-containing ligands as well as ca. 60 PEGylated ligands used to enhance water solubility of the entire NP. The maleimide-derivatized AuNPs can be generated via a thermal retro Diels–Alder reaction, and then subsequently reacted with thiol/amine bearing compounds via the highly efficient Michael addition. AuNPs thus prepared can, for example, be derivatized with ^{18}F-labeled SiFA-SH, a radiolabeling prosthetic group,[12,13] and/or peptides such as the somatostatin receptor targeting peptide cys-tyr^3-octreotate (cys-TATE). Labeling of the AuNPs enables the use of small animal positron emission tomography (PET), a noninvasive diagnostic imaging modality, to assess the biodistribution of AuNP in general and determine the extent of BBB transfer in a rat model, most likely by adsorptive transcytosis. In the course of our study, a related study was conducted by Albericio and Kogan.[14] Their results showed that a relatively large AuNP template (12 nm Au core, modified with [^{18}F]fluorobenzoate) has a similar in vivo distribution as that reported by DeJong et al.[9] and Kreyling et al.,[10] with an insignificant quantity of brain uptake measured. The main goal of this study was thus to explore the benefits of the efficient maleimide/thiol click chemistry for AuNP derivatization and to devise a simple ^{18}F-labeling protocol for potential applications in positron emission tomography (PET). Furthermore, we investigated the in vivo biodistribution of ^{18}F-labeled AuNP by small animal PET. The preliminary PET results reveal that the partially hydrolyzed [^{18}F]SiFA-maleimide-AuNPs ([^{18}F]**8**) shows significantly higher brain uptake (> 0.13 %ID/g) compared to the nonhydrolyzed [^{18}F]SiFA-maleimide-AuNPs ([^{18}F]**6**) (0.07 %ID/g). This simple, highly efficient maleimide–thiol radiolabeling procedure can be easily adapted to other NP systems.

RESULTS AND DISCUSSION

Synthesis of the Maleimide-AuNP. The 3 nm water-soluble PEGylated AuNP template (1) (Scheme 1) was prepared via a revised Brust-Schiffrin two-phase method using a 3:1 thiol:hydrogen tetrachloroaurate with TOAB, and further reduced in a large excess of tetrabutylammnonium borohydride (Bu_4NBH_4, 11.3-fold). A short chain (n = 3) hydroxy-terminated PEG thiol was used to provide water solubility of

dx.doi.org/10.1021/bc5001593 | Bioconjugate Chem. 2014, 25, 1143–1150

AuNPs and to facilitate the purification after AuNP formation. A furan masked maleimide−PEG-thiol (**2**) was then attached to PEGylated-AuNP surface using PEGylated thiol **1**:**2** in a 1:1 ratio for 1h via a place-exchange reaction yielding furan protected AuNP (**3**) (Scheme 1). We initially reported that the maleimide functional group can be recovered by heating **3** at elevated temperatures in water or buffer and introduced to subsequent Michael addition chemistry.[11] However, this is an error as was shown by Gobbo and Workentin, under the conditions reported (aqueous solutions at elevated temperatures) some of the maleimide functionalities do in fact hydrolyze, resulting in the ligand shell of the NP (prior to Michael addition reaction) being a mixure of intact maleimide ligands, hydrolyzed ligands, and PEGylated ligands.[15] Post-reaction purification does however remove the hydrolyzed ligand, as was demonstrated.[11] Because the furan-protected maleimide AuNPs (**3**) demonstrate excellent solubility in anhydrous DMSO, hydrolysis can be readily circumvented by performing the retro Diels−Alder deprotection in anhydrous DMSO. ^{1}H NMR spectra show that the deprotected maleimide can be quantitatively generated after heating **3** in DMSO at 95 °C for 2 h (Supporting Information, Figure S1).

Cytotoxicity Test of Maleimide-AuNP and PEGylated AuNP. The cytotoxicity of the maleimide derivatized AuNPs (**4** and **7**) was assessed by exposing HeLa cells to these AuNP followed by an MTT assay (3-(4,5-dimethylthiazol-2-yl)-2,5-diphenyltetrazolium bromide).[16] The maleimide-AuNPs exhibit negligible toxicity toward HeLa cells at low to moderate concentrations (<0.1 mM), and only limited toxicity at high (0.1−1.0 mM) concentrations (Supporting Information, Figure S2).

Bioconjugation and Characterization of Maleimide-AuNP with [^{18}F]SiFA-SH. Preliminary in vivo biodistribution studies of AuNPs (containing either hydrolyzed and/or non-hydrolyzed maleimide moieties) were performed by labeling the AuNPs (4 and **7**) with the positron emitter ^{18}F ($t_{1/2}$ = 109.98 min). Positron emitters such as ^{68}Ga, ^{64}Cu, ^{86}Y, and ^{89}Zr have previously been linked to various NP surfaces, including quantum dots, iron oxide NPs, polymer NPs, and lipid NPs.[1] One major drawback of these NP complexes is that the radiolabeled chelators are usually non-covalently adsorbed onto the NP surface, rather than covalently bound. This can lead to a detachment of the radioligand from the NP surface in vivo. A covalent binding strategy to radiolabel or load the AuNPs with a molecular cargo is therefore preferable in regard to in vivo stability. For facile ^{18}F-labeling, an ^{18}F labeled prosthetic group, thiol (4-(di-*tert*-butylfluorosilanyl)benzenethiol ([^{18}F]SiFA-SH, [^{18}F]**5**), was first synthesized (Scheme 1).[12,13] The SiFA chemistry, which is dependent on silicon-^{18}F bond formation, is one of several novel ^{18}F-labeling methods based on boron, aluminum, and silicon labeling chemistry.[17−19] SiFA-SH (**5**) was conveniently labeled through a fast isotopic exchange reaction with ^{18}F$^-$ in one step prior to the AuNP labeling (Supporting Information Figure S4.a). [^{18}F]**5** was subsequently conjugated to the maleimide-AuNPs (**4** and **7**) via a Michael addition reaction (Scheme 1 and SI Figure S3.b). A freshly prepared solution of **5** was necessary for each conjugation reaction because disulfide formation occurs over time. The most significant advantage of this AuNP labeling technique is that it combines maleimide/thiol click chemistry with the SiFA labeling methodology,[20] yielding [^{18}F]**5** in a single step without the necessity of HPLC purification. The final purification of the SiFA-labeled AuNPs ([^{18}F]**6** and [^{18}F]**8**) can be achieved without HPLC purification as well, owing to the large size difference between SiFA-labeled AuNPs and the low molecular weight SiFA-SH. The use of a single size-exclusion gel cartridge is sufficient to collect pure [^{18}F]**6** and [^{18}F]**8** with an overall radiochemical yield (RCY) of 60−87% within a very short time (Supporting Information, Figure S3.c). The characteristic black-brown color of AuNPs on the gel enables the visual collection of the AuNP fraction. The entire labeling and purification process can be achieved within 25 min, which is especially compatible with the short-lived ^{18}F radioisotope ($t_{1/2}$ = 109.98 min) used in PET imaging (Supporting Information, Scheme S1).

To establish that [^{18}F]**5** was covalently bound to the AuNP surface instead of being only physically adsorbed, [^{18}F]SiFA-OH, which closely resembles SiFA-SH structurally but lack the Michael donor reactive group, was mixed with the maleimide-AuNPs (**7**) under the same coupling conditions for 10 min. After work-up, no radioactivity was detected in the AuNP fraction. A similar control experiment using [^{18}F]**5** was also carried out with furan protected maleimide-AuNPs (**3**) following the same labeling protocol. Moreover, no detectable radioactivity was found in the AuNP fraction after work-up, indicating that no thiol-for-thiol exchange reaction on the AuNP surface occurred during the labeling procedure.

To take advantage of the high sensitivity of PET, only three [^{18}F]**5** molecules on average (as calculated from stoichiometry) were introduced onto each AuNP. To further confirm the conjugation of SiFA-SH to the maleimide-AuNP surface, X-ray photoelectron spectroscopy (XPS) spectra of the maleimide-AuNP (**4**) before and after the Michael addition reaction with **5** were obtained (Figure 1). The appearance of the F 1s peak at 686.8 eV in the SiFA-maleimide-AuNP sample and its absence in the maleimide-AuNP sample indicates that the Michael addition reaction with **5** was successful.

Small Animal PET Study of [^{18}F]SiFA Labeled Maleimide-AuNP. The maleimide-AuNPs carry multiple-maleimide functional group (30 per nonhydrolyzed maleimide-AuNP) offering a versatile platform for the development of nanobased diagnostics and therapeutics. These have the potential to carry a drug of choice as well as a radioactive tag to determine its spatial and temporal in vivo distribution. To evaluate the biodistribution of the radiolabeled and carrier loaded AuNPs and their ability to cross the BBB, [^{18}F]**5** labeled maleimide-AuNPs ([^{18}F]**6**) (3 SiFAs per AuNP) were intravenously injected into healthy rats (n = 3) and dynamic microPET images were acquired over the subsequent 120 min. As an in vivo control experiment, pure [^{18}F]**5** alone was injected into rats under similar conditions to assess its ability to cross the BBB independent of the AuNP carrier. The pure [^{18}F]**5** without the AuNP carrier was incapable of crossing the rat BBB, probably as a result of its high lipophilicity or strong binding to serum proteins. Figure 2 shows the summed PET images of [^{18}F]**5** (Figure 2a−c) and ^{18}F-labeled AuNP [^{18}F]**6** (Figure 2d−f) in rat brain after 120 min. [^{18}F]**6** shows a very limited ability to accumulate in the brain with only 0.07%ID/g (percentage injected dose per gram of tissue) (Figure 2d−f).

However, the adventitious hydrolysis of the maleimide prior to the desired Michael addition reaction also proved to be most fortuitous, as residual carboxylates in the ligand shell enhance BBB transfer. As the hydrolysis of the maleimide groups is inevitable in aqueous media[15] we deliberately allowed for the hydrolysis some of the maleimide in the maleimide-AuNPs. The controlled hydrolysis was carried out by adding water

dx.doi.org/10.1021/bc5001593 | *Bioconjugate Chem.* 2014, 25, 1143−1150

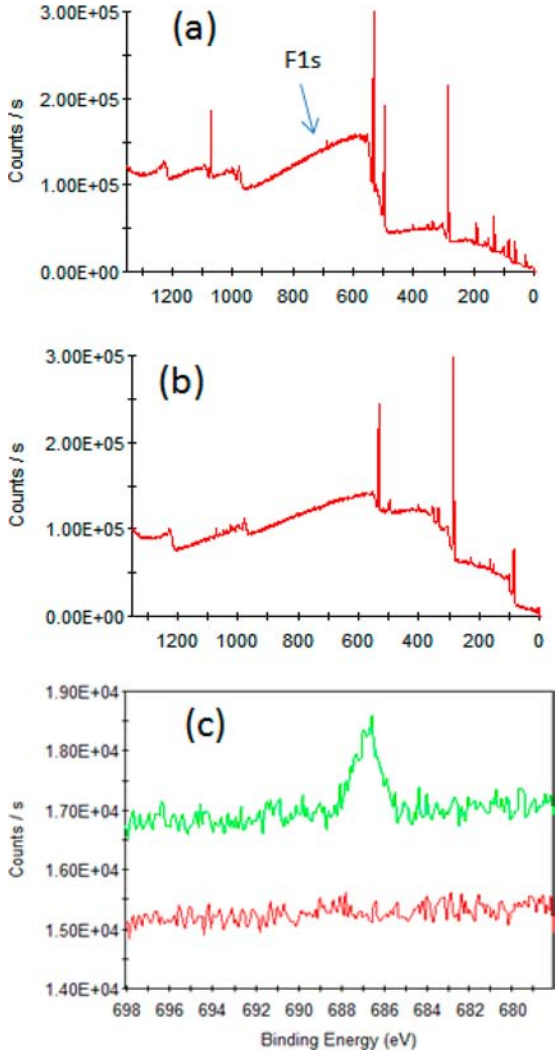

Figure 1. X-ray photoelectron spectra of (a) SiFA-maleimide-AuNP (**6**); (b) maleimide-AuNP (**4**); and (c) offset high resoultion F 1s scans of SiFA-maleimide-AuNP (**6**, green) and maleimide-AuNP (**4**, red).

(20% of the total volume) to the anhydrous DMSO solution after the retro-Diels–Alder reaction of AuNP (**3**). Heating was continued for 2 h to produce AuNP (**7**). After partial hydrolysis,[21] the Michael addition reaction of **7** with 3 equiv of [^{18}F]**5** could still be quantitatively performed indicating the availability of sufficient number of intact maleimides.[22] The resulting partially hydrolyzed [^{18}F]**8** were evaluated by microPET in rats (n = 3) using the identical imaging protocol as for [^{18}F]**6**. The effect of introducing carboxylate moieties in the mixed ligand shell of PEG and SiFA-maleimide on BBB crossing is readily discernible: [^{18}F]SiFA-maleimide-carboxylate AuNPs ([^{18}F]**8**) show a higher brain uptake in the PET scan than that of [^{18}F]**6** (Figure 2g,h,i) (%ID/g value of 0.13 vs 0.07 of [^{18}F]**6**). The time–activity curves of the brain distribution of [^{18}F]**8** obtained from the PET images show the accumulation of radiolabeled AuNP ([^{18}F]**8**) in the cerebellum and brain with time (Figure 3), using muscle as the reference tissue. Unlike larger NPs (e.g., 12 nm NPs),[14] the derivatized and partially hydrolyzed 3 nm NPs exhibit continuing increase of radioactivity accumulation in the cerebellum and brain over 120 min.

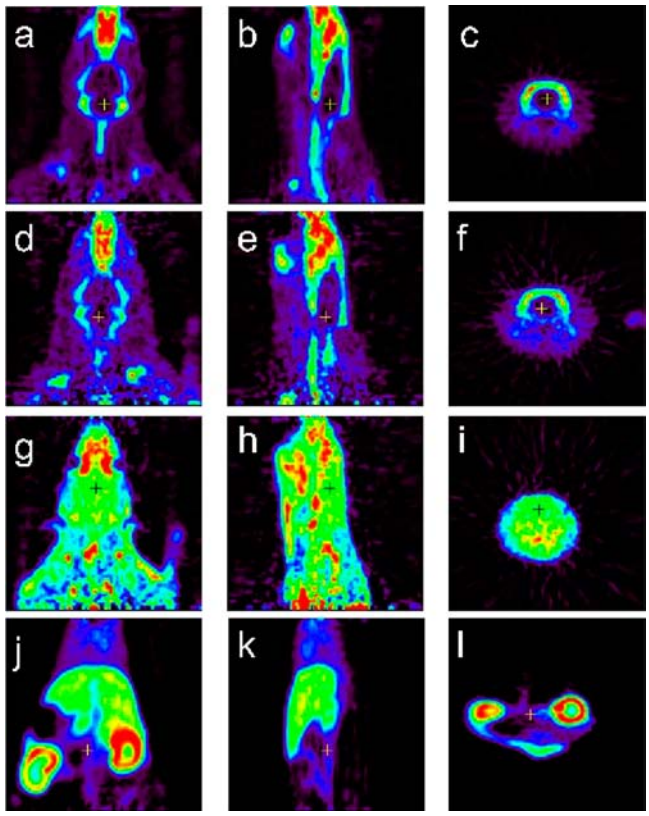

Figure 2. Representative images of microPET scans of rat brain after intravenous injection of [^{18}F]SiFA-SH ([^{18}F]**5**) (a,b,c), [^{18}F]SiFA-maleimide-AuNPs ([^{18}F]**6**) (d,e,f), and partially hydrolyzed [^{18}F]-SiFA-maleimide-AuNPs ([^{18}F]**8**) (g,h,i). Brain scan images in coronal (a,d,g), sagittal (b,e,h), and transverse planes (c,f,i); sum images t = 120 min. Body scan images of partially hydrolyzed [^{18}F]-SiFA-maleimide-AuNP ([^{18}F]**8**) in coronal (j), sagittal (k), and transverse planes (l) (sum images t = 60 min).

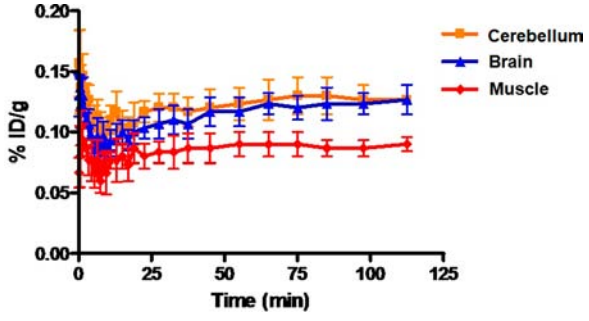

Figure 3. Time-activity curves for cerebellum, brain, and muscle uptake extracted from in vivo microPET scans of partially hydrolyzed [^{18}F]SiFA-maleimide-AuNPs ([^{18}F]**8**). Each data point represents the average of three independent animal experiments. The error bars are expressed as SEM (n = 3). %ID/g is the percentage of injected dose per gram of tissue.

A static whole body sum PET image of [^{18}F]**8** was acquired after 1 h to identify the main pathway of excretion (Figure 2j,k,l). Uptake in the kidneys, liver, and spleen were the highest with %ID/g values of 2.15, 1.70, and 1.65, respectively. The high concentration in the kidneys indicates renal clearance of [^{18}F]**8**, while the high concentration in the liver and spleen suggest a hepatic clearance and excretion via the reticuloendothelial system (RES). Detached ^{18}F$^-$ originating from the SiFA

dx.doi.org/10.1021/bc5001593 | Bioconjugate Chem. 2014, 25, 1143–1150

tag would result in a radioactivity accumulation in bone. As demonstrated by us and others, the SiFA group bearing the ^{18}F is stable toward in vivo hydrolysis and the radioactivity uptake in bone was therefore minimal providing a general labeling strategy for maleimide derivatized NPs. The cerebellum and brain ROIs have a %ID/g value about 70% higher than muscle, which makes this **7** a promising platform for the development of a transport carrier for in vivo PET tracers lacking the ability to traverse the BBB by themselves.

Ex Vivo Biodistribution of [^{18}F]SiFA-AuNP ([^{18}F]8) in Rats. Ex vivo measurements (n = 3) subsequent to the in vivo PET measurements confirmed the time-dependent PET data (Supporting Information, Figure S5). It is noteworthy that, from the ex vivo data, the cerebellum and brain have %ID/g values of about 0.14 (after thorough perfusion to eliminate blood radioactivity in the brain), in agreement with the PET image data analysis, while the muscle and bone have the lowest %ID/g value of about 0.08. A long-term study of the excretion routes of labeled AuNP **8** could not be performed due to the short half-life of ^{18}F ($t_{1/2}$ = 109.98 min). To this end a study using ^{64}Cu ($t_{1/2}$ = 12 h) as a long-lived radionuclide is planed.

PET tracers in clinical use which pass the BBB by passive transport targeting brain receptors generally show a brain uptake from 0.1 %ID/g (lower threshold) to 1−2%ID/g; [^{18}F]**8** as represented here has an uptake of 0.13 %ID/g. As a result of the low resolution of PET technology (2 mm spatial resolution), there is no direct evidence proving that the detected radioactivity in the brain ROI (region of interest) is caused by the nanoparticles present in the brain parenchyma or the BBB. A TEM (transmission electron microscopy) study of brain slices might be able to clarify this question. However, a previous study from Guerrero et al. using a large 12 nm [^{18}F]fluorobenzoate-labeled peptide coated AuNPs showed that the radioactivity level in brain decreased over time.[14] This was attributed to the clearance of the AuNPs from the blood vessels.[14] Our PET study, however, showed that the radioactivity level of the small 3 nm maleimide-AuNP ([^{18}F]**8**) in brain slightly increases over time, indicating a dynamic active transport mechanism.

Small Animal PET Study of Dual Conjugated Maleimide-AuNP with cys-TATE (9) and [^{18}F]SiFA-SH ([^{18}F]5). Peptide based imaging agents are of growing importance in oncologic PET imaging and could benefit from association with nanoparticles to potentially enhance cooperative binding to target receptor systems. The results of the PET experiments described above with the maleimide derivatized AuNPs suggest that it may be possible to introduce other thiol/amine functionalized molecules (e.g., peptides) on to the AuNP surface through the same Michael addition reaction in conjugation with the [^{18}F]SiFA label for radioactivity detection. As a proof-of-concept, a cysteine derivatized TATE peptide (cys-TATE, **9**, a peptide binding to the somatostatin receptor found on endocrine tumors) was synthesized and conjugated coincidentally with [^{18}F]**5** and cys-TATE (**9**) onto the partially hydrolyzed maleimide-AuNPs (**7**) (3 equiv of [^{18}F]SiFA and 3 equiv of cys-TATE) (Scheme 1). The different electrophoretic migration patterns of **7**, **8**, and **10** on agarose gel during electrophoresis establish that the peptide **9** and **5** could be successfully conjugated to the maleimide-AuNP surface (Supporting Information, Figure S6). Preliminary microPET studies (n = 3) showed that [^{18}F]**10** accumulates in the brain ROI with a similar efficiency as [^{18}F]**8** (Supporting Information, Figure **S7**). These results are very encouraging since one could incorporate different thiol containing tags, in this case a peptide (cys-TATE) and a radiolabeled prosthetic group (^{18}F-SiFA-SH) via the same Michael addition reaction. In this particular preliminary study we were primarily interested in establishing a working protocol to efficiently load the NPs with different compounds. Further studies are required to assess the binding of TATE tethered ^{18}F-labeled AuNPs in an appropriate animal tumor model. We are currently evaluating the binding of TATE decorated AuNPs to somatostatin expressing cell lines and plan related in vivo tumor imaging.

CONCLUSION

In summary, ^{18}F-radiolabeled AuNPs (nonhydrolyzed and partially hydrolyzed) can be quickly synthesized and readily purified in high radiochemical yields (60−80%) using the SiFA labeling methodology. The covalent ^{18}F-labeling procedure based on maleimide/thiol click chemistry provides stable radionuclide attachment to the AuNP. The labeling protocol does not require complicated HPLC purification and relies solely on solid phase based techniques. In addition to the radioactive tag, a bioactive peptide was conjugated to the same AuNPs in a proof of concept experiment. This offers a general protocol to derivatize AuNPs with thiol bearing molecules and concomitantly follow the in vivo biodistribution of these AuNPs via PET imaging. The AuNPs prepared herein were subjected to a preliminary small animal PET study in healthy rats, provides information about their excretion pathways and accumulation in various organs. The partially hydrolyzed AuNPs in particular accumulate in the brain (0.13 %ID/g) as indicated by the brain PET images and corroborated by ex vivo investigation of the fully perfused brain. However, further studies are required in order to clarify exact location of these NP in the brain as well as the mechanism of uptake. Future experiments using targeting ligands as well as surface modifiers such as cell penetrating peptides or ligands binding to surface receptors of the BBB will further optimize and extend the usefulness of this promising bioconjugation platform for in vivo applications.

EXPERIMENTAL SECTION

Commercial Solvents and Reagents. Potassium tetrabromoaurate (III), hydrogen tetrachloroaurate (III), tetraoctylammonium bromide, tetrabutylammonium borohydride, triethylene glycol, carbon tetrabromide, triphenyl phosphine, furan, maleimide, potassium thioacetate, thiourea, and cysteine were all purchased from Aldrich and used as received. 4-(Di-*tert*-butylfluorosilanyl)benzenethiol (SiFA-SH) was synthesized following the reference procedure.[12,13,20] Potassium carbonate (Caledon), chloroform-d_6 (Cambridge Isotope Laboratories), and D_2O (Cambridge Isotope Laboratories) were also used as received.

General Instrumentation. ^{1}H NMR spectra and ^{13}C NMR spectra were recorded on Varian 300 (300 MHz) and Inova 500 (500 MHz) spectrometers in deuterated chloroform, or deuterated hydrogen oxide solutions, and are reported in parts per million (ppm), with the residual protonated solvent resonance used as a reference. HR-MS (electrospray ionization, ESI) analyses were recorded from the MS facility of the Department of Chemistry of McGill University. Infrared spectra were recorded on a PerkinElmer ATR-FTIR spectrometer and are reported in wavenumbers (cm^{-1}). X-ray photoelectron spectroscopy was collected using a VG

dx.doi.org/10.1021/bc5001593 | Bioconjugate Chem. 2014, 25, 1143−1150

ESCALAB 220i-XL spectrometer employing a monochromatic A1KR X-ray source and a hemispherical electrostatic analyzer. Radio-TLC plates were assessed by a Rayrest Radio-TLC miniGITA reader.

Synthesis of Furan Protected Maleimide AuNP (3). The furan protected maleimide AuNP (**3**) was prepared as described previously, via a place exchange reaction of PEGylated AuNP (**1**) with 2-(2-(2-(2-mercaptoethoxy)-ethoxy)ethyl)-3*a*,4,7,7*a*-tetrahydro-1*H*-4,7-epoxyisoindole-1,3(2*H*)-dione (**2**).[11] Briefly, PEGylated AuNP (**1**) was prepared via a revised Brust-Schiffrin method. Potassium tetrabromoaurate(III) (0.30 g, 0.54 mmol) or hydrogen tetrachloroaurate trihydrate (0.21 g, 0.54 mmol) was dissolved in Milli-Q water (20 mL), and mixed with tetraoctylammonium bromide (TOAB, 0.36 g, 0.65 mmol) in toluene (200 mL). The contents were vigorously stirred for 30 min at room temperature to facilitate the phase transfer of the gold(III) into the toluene layer, resulting in the organic layer turning dark orange and the aqueous layer becoming clear and colorless. The aqueous layer was removed, and the organic layer dried with $MgSO_4$ and filtered. The resulting solution was cooled to 0 °C in an ice bath, 3 equiv of thiol **2** (TEG-thiol, 0.27 g, 1.64 mmol) in isopropanol (10 mL) were added via a volumetric pipet, and the solution was allowed to stir for 10 min. The orange color faded with time. A fresh solution of tetrabutylammonium borohydride (1.40 g, 5.45 mmol) in isopropanol (10 mL) was added to the rapidly stirring toluene solution over 5 s. The solution turned dark black instantly. The PEGylated nanoparticles (**1**) started to precipitate from toluene after 2 h. After stirring the mixture overnight (~12 h), 30 mL of Milli-Q water was added under moderate stirring to extract the PEGylated AuNP (**1**). The black aqueous layer was transferred into a dialysis tube (1000 Da cutoff) and dialyzed in 3 L of Milli-Q water for 3 days; the dialysis water was changed every 10 h. The resulting AuNP (**1**) sample was collected after lyophilization. The resulting PEGylated AuNP (**1**) was dark brown in color.

The furan-protected maleimide AuNP (**3**) was then prepared following the standard place-exchange reaction of thiol **2** with the PEGylated AuNP (**1**). A typical procedure involved mixing the previously prepared PEGylated NP (**1**) (100 mg, 0.5 μmol, about 48 μmol of PEGylated ligands) and thiol **2** (15 mg, 48 μmol). The mixed ligand AuNP (**3**) material was then purified by washing with acetonitrile, isoproponal, and toluene. ^{1}H NMR spectroscopy was used to characterize and check the purity of the AuNP (**3**). (SI Figure S1.i).

General Procedures for the Preparation of Maleimide-AuNP (4) and Partially Hydrolyzed Maleimide-AuNP (7). The maleimide-AuNP can be generated in either nonhydrolyzed (**4**) and partially hydrolyzed (**7**) forms. The hydrolysis is known to be highly pH and temperature dependent.[21,23] Generally, the nonhydrolyzed maleimide-AuNP (**4**) can be generated by heating at 95 °C in anhydrous DMSO for 2 h as monitored by ^{1}H NMR spectroscopy. The partially hydrolyzed sample (**7**) can be produced by continuous heating at 95 °C after adding 20% (volume percentage) of Milli-Q water to the DMSO solution, for 2 h. Fresh maleimide-AuNP (**4** or **7**) samples were generated immediately before the Michael addition reaction was performed.

Cytotoxicity Test of PEGylated AuNP (1) and Maleimide-AuNPs (4, 7). The cytotoxicity test was carried out by exposing a HeLa cell culture to the prepared AuNPs (**1**, **4**, **7**) and quantifying the effect of the NPs by determining the IC_{50} values in MTT(3-(4,5-dimethylthiazol-2-yl)-2,5-diphenyl-tetrazolium bromide) assays.[16] Briefly, 10^4 HeLa cells were seeded on each well of a 96-well plate in 180 μL of DMEM media with 10% fetal calf serum and incubated at 37 °C with 5% CO_2 for 24 h. The cells were then treated with 20 μL AuNPs at different concentrations (0.00125−2.0 mM). Cells without treatment were used as a negative control. The maleimide-AuNP (**4**), partially hydrolyzed maleimide-AuNP (**7**), and PEGylated AuNP (**1**) remain stable under all test concentrations after addition to the cell culture for 6 days, as indicated by the permanence of the brownish color. Destabilization would be indicated by the precipitation of AuNPs and a fading of the color in the cell culture. After 6 days, the medium was removed, and cells were washed with PBS for 3 times and then incubated with 100 μL of fresh culture medium in addition to 30 μL of freshly made 5 mg/mL MTT solution at 37 °C in 5% CO_2 for 4 h. 100 μL lysis buffer (50 mL 100% Triton X-100 and 2 mL 12 M HCl in 448 mL isopropanol) per well was added. Cells were further incubated overnight and the absorbance was measured at 550 nm (with reference 690 nm) using a Synerg4 spectrophotometer (Biotek). In comparison with PEGylated AuNP (**1**), the maleimide derivatized ligand of AuNP (**4**, **7**) did not exhibit prominent toxicity toward HeLa cells. The IC_{50} value for the maleimide-AuNP is about 0.5 mM, similar to that of the PEGylated AuNP.

Radiolabeling of Maleimide-AuNP (4) with [^{18}F]SiFA-SH (5). 4-(Di-*tert*-butylfluorosilanyl)benzenethiol (SiFA-SH) (**5**) was synthesized following a reference procedure.[12,13,20] [^{18}F]Fluoride/H_2[^{18}O]O (1.11 GBq, 30 mCi in 0.5 mL H_2[^{18}O]O) was passed through a QMA cartridge preconditioned with 1 M potassium carbonate (10 mL) and H_2O (10 mL). The trapped $^{18}F^-$ was then eluted from the cartridge with 1 mL of a stock solution of Kryptofix2.2.2 (75 mg, 0.20 mmol) and potassium oxalate (18.4 mg, 0.10 mmol) in 96/4 acetonitrile/H_2O solution (10 mL). The water was azeotropically removed by coevaporation with anhydrous CH_3CN (3 × 1 mL) using a stream of nitrogen at 100 °C. The dried [^{18}F]F^-/Kryptofix 2.2.2/K^+ complex was dissolved in anhydrous CH_3CN (0.3 mL). SiFA-SH (**5**) (20 μg, 74 nmol) in dry CH_3CN (0.2 mL) was added and reacted at room temperature for 10 min. The radiochemical yield of [^{18}F]SiFA-SH ([^{18}F]**5**) was determined by radio-TLC (hexane:ethyl acetate:TFA = 95:5:1) to be in the range of 60−85% without decay correction. This [^{18}F]SiFA-SH/CH_3CN solution was used for maleimide-AuNP (**4**) labeling without further purification.

Furan protected maleimide-AuNP (**3**, 4 mg, 18.2 nmol, 30 maleimide ligands and 60 PEG ligands on each NP) were dissolved in anhydrous DMSO (0.4 mL). The maleimide end group was recovered by heating the solution at 95 °C for 2 h to yield AuNP (**4**) as described above. To this solution, 0.38 mL of [^{18}F]**5** (54.6 nmol) as obtained above was added and reacted with maleimide-AuNP (**4**) at room temperature for 10 min. The [^{18}F]SiFA-AuNP (**6**) could be readily purified by passing the solution through a NAP-10 size exclusion column (SEC, equilibration buffer: 0.1 M sodium PBS, pH 7.2) where the black eluate (first fraction) was collected. The purity of the product was confirmed by radio-TLC (hexane:ethyl acetate:TFA = 95:5:1) as [^{18}F]**6**.

Radiolabeling of Partially Hydrolyzed Maleimide-AuNP (7) with [^{18}F]-SiFA-SH (5). A controlled hydrolysis reaction was carried out after deprotection of the furan protected maleimide-AuNP (**3**, 4 mg, 18.2 nmol) in 0.4 mL

dx.doi.org/10.1021/bc5001593 | *Bioconjugate Chem.* 2014, 25, 1143−1150

anhydrous DMSO. Distilled water (0.1 mL) was added to the mixture and heating was continued at 95 °C for 2 h. [^{18}F]SiFA-SH (**5**) was reacted with the remaining maleimides on the AuNP surface with the same labeling efficiency (AuNP(**7**)/[^{18}F]**5** = 1:3) as the labeling of AuNP (**4**). Radio-TLC (hexane:ethyl acetate:TFA = 95:5:1) of the crude mixture confirmed that the [^{18}F]SiFA-SH (**5**) reacted quantitatively with the partially hydrolyzed AuNP (**7**) with the same stoichiometry. The partially hydrolyzed ^{18}F-labeled AuNP ([^{18}F]**8**) were separated by the same SEC method (cf. S4) and radio-TLC (hexane:ethyl acetate:TFA = 95:5:1) was used to confirm its purity. The [^{18}F]SiFA-AuNP ([^{18}F]**8**) was kept in a shielded container for 24 h until it had decayed sufficiently for XPS analysis.

Reaction of Cysteine-Modified TATE Peptide (cys-TATE, 9) with Maleimide-AuNP (7). To test the reactivity of cysteine-modified TATE (cys-TATE, **9**) with the partially hydrolyzed maleimide-AuNP (**7**) via the Michael addition reaction, **7** (prepared following the same procedure as described above) was mixed with cys-TATE (**9**, 54.6 μg, 54.6 nmol) and the resulting TATE-AuNP (**11**) was purified by SEC (equilibration buffer: 0.1 M sodium PBS, pH 7.2). The coupling of cys-TATE to AuNP (**7**) was confirmed by gel electrophoresis.

Conjugation of cys-TATE (9) and [^{18}F]SiFA-SH ([^{18}F]5) to Maleimide-AuNP (7). Cys-TATE (54.6 μg, 54.6 nmol) and [$^{18/19}$F]**5** (15 μg, 54.6 nmol; 12−16 mCi, cf SI Figure S4) were mixed in a 1:1 ratio and introduced onto partially hydrolyzed maleimide-AuNP (**7**). [^{18}F]**5** and cys-TATE (**9**) were reacted with partially hydrolyzed maleimide-AuNP (**7**) at room temperature for 10 min. No unreacted [^{18}F]**5** was detected by radio-TLC which confirmed the completion of the reaction. The product AuNP ([^{18}F]**10**) was purified by SEC (equilibration buffer: 0.1 M sodium PBS, pH 7.2) and its purity was confirmed by radio-TLC. The final radiochemical yield was 60−80% without decay correction. Electrophoresis was carried out after allowing [^{18}F]**10** to decay sufficiently behind shielding.

Small Animal PET Imaging in Rats. Sprague−Dawley rats for in vivo PET studies were housed in a 12 h light/dark cycle at 21 °C with access to food and water ad libitum, treatment according to the Guide to the Care and Use of Experimental animals (Ed2) of the Canadian Council on Animal Care. The MicroPET imaging protocol was approved by the Animal Care Committee of McGill University (Montreal, Canada). The rats were kept under isoflurane anesthesia for the injection of the ^{18}F labeled AuNPs and [^{18}F]SiFA-SH (**5**). Respiration rate, heart rate, and body temperature were monitored throughout the scan (Biopac systems MP150, Goleta, CA, USA). 12−15 MBq (0.32−0.40 mCi) of ^{18}F labeled [^{18}F]SiFA-SH (**5**), as well as the AuNP ([^{18}F]**6**, [^{18}F]**8**, and [^{18}F]**10**) were intravenously administered via a lateral tail vein. Brain scan data were acquired for 2 h using a Concord MicroPET R4 small animal tomograph. All images were reconstructed using filtered back projection after applying normalized scatter correction for attenuation and radioactive decay. The PET images were analyzed using ASIPRO software (Concorde Microsystems).

Ex Vivo Biodistribution of [^{18}F]SiFA-AuNP ([^{18}F]8) in Rats. 12−15 MBq (0.32−0.40 mCi) of [^{18}F]**8** was intravenously administered via a lateral tail vein into Sprague−Dawley rats (n = 3). Whole body biodistribution data of [^{18}F]**8** were acquired for 1 h and brain data were acquired for 2 h in a dynamic acquisition mode. The time-activity curves were obtained from regions of interest in cerebellum and brain using muscle as the reference tissue.

The SD rats were sacrificed after the PET scan (2 h postinjection of [^{18}F]**8**). The organs were removed, rinsed with physiological saline, blotted dry, and placed in preweighed tubes. The radioactivity in each tube was counted in a gamma counter (Cobra II, Packard Instruments) and used to calculate the percentage of the injected dose per gram of tissue (% ID/g) for each organ. The mean results from three rats are reported here (Figure S5).

■ ASSOCIATED CONTENT

Supporting Information

Cytotoxicity data, NMR, radio-TLC, ex vivo biodistribution, and electrophoresis data. This material is available free of charge via the Internet at http://pubs.acs.org.

■ AUTHOR INFORMATION

Corresponding Authors

*Fax: +1 514-340-7502; Tel: +1-514-398-1857; E-mail: ralf.schirrmacher@mcgill.ca.

*Fax: +1 514-398-3797; Tel: +1-514-398-5244; E-mail: bruce.lennox@mcgill.ca.

Notes

The authors declare no competing financial interest.

■ ACKNOWLEDGMENTS

The authors thank Mr. Antonio Aliaga for technical assiatance with the PET imaging experiments. This work was supported by grants from CHIR (RS), NSERC (RS, RBL) and FQRNT (RBL).

■ REFERENCES

(1) Liu, Y., and Weich, M. J. (2012) Nanoparticles labeled with positron emitting nuclides: advantages, methods, and applications. *Bioconjugate Chem. 23*, 671−682.

(2) Gunasekera, U. A., Pankhurst, Q. A., and Douek, M. (2009) Imaging applications of nanotechnology in cancer. *Target Oncol. 4*, 169−181.

(3) Weissleder, R. (2006) Molecular imaging in cancer. *Science 312*, 1168−1171.

(4) Liu, X., Liu, H., Zhou, W., Zheng, H., Yin, X., Li, Y., Guo, Y., Zhu, M., Ouyang, C., Zhu, D., and Xia, A. (2010) Thermoreversible covalent self-assembly of oligo(p-phenylenevinylene) bridged gold nanoparticles. *Langmuir 26*, 3179−3185.

(5) Thode, C. J., and Williams, M. E. (2008) Grignard functionalization of Weinreb amide modified Au nanoparticles. *Langmuir 24*, 5988−5990.

(6) Sommer, W. J., and Weck, M. F. (2007) Facile functionalization of gold nanoparticles via microwave-assisted 1,3 dipolar cycloaddition. *Langmuir 23*, 11991−11995.

(7) Li, X.-M., Huskens, J., and Reinhoudt, D. N. (2004) Reactive self-assembled monolayers on flat and nanoparticle surfaces, and their application in soft and scanning probe lithographic nanofabrication technologies. *J. Mater. Chem. 14*, 2954−2971.

(8) Weintraub, K. (2013) Biomedicine: The new gold standard. *Nature 495*, S14−S16 and reference therein..

(9) De Jong, W. H., Hagens, W. I., Krystek, P., Burger, M. C., Sipsb, A. J. A. M., and Geertsma, R. E. (2008) Particle size-dependent organ distribution of gold nanoparticles after intravenous administration. *Biomaterials 29*, 1912−1919.

(10) Lipka, J., Semmler-Behnke, M., Sperling, R. A., Wenk, A., Takenaka, S., Schleh, C., Kissel, T., Parak, W. J., and Kreyling, W. G. (2010) Biodistribution of PEG-modified gold nanoparticles following

intratracheal instillation and intravenous injection. *Biomaterials 31*, 6574−6581.
(11) Zhu, J., Waengler, C., Lennox, R. B., and Schirrmacher, R. (2012) Preparation of water-soluble maleimide-functionalized 3 nm gold nanoparticles: a new bioconjugation template. *Langmuir 28*, 5508−5512.
(12) Wängler, B., Kostikov, A. P., Niedermoser, S., Chin, J., Orchowski, K., Schirrmacher, E., Iovkova-Berend, L., Jurkschat, K., Wängler, C., and Schirrmacher, R. (2012) Protein labeling with the labeling precursor [^{18}F]SiFA-SH for positron emission tomography. *Nat. Protoc. 7*, 1964−1969.
(13) Wängler, B., Quandt, G., Iovkova, L., Schirrmacher, E., Wangler, C., Boening, G., Hacker, M., Schmoeckel, M., Jurkschat, K., Bartenstein, P., and Schirrmacher, R. (2009) Kit-like ^{18}F-labeling of proteins: synthesis of 4-(Di-*tert*-butyl[^{18}F]fluorosilyl)benzenethiol (Si[^{18}F]FA-SH) labeled rat serum albumin for blood pool imaging with PET. *Bioconjugate Chem. 20*, 317−321.
(14) Guerrero, S., Herance, J. R., Rojas, S., Mena, J. F., Gispert, J. D., Acosta, G. A., Albericio, F., and Kogan, M. J. (2012) Synthesis and in vivo evaluation of the biodistribution of a 18F-Labeled conjugate gold-nanoparticle-peptide with potential biomedical application. *Bioconjugate Chem. 23*, 399−408.
(15) Gobbo, P., and Workentin, M. S. (2012) Improved methodology for the preparation of water-soluble maleimide-functionalized small gold nanoparticles. *Langmuir 28*, 12357−12363 These authors present an alternative PEG-thiol (a methylether-terminated triethylene glycerol thiol) and an alternative furan-protected tetraethylene glycerol thiol to that used in ref 11. The resulting PEGylated-AuNP are soluble in toluene and can be thermally deprotected in the absence of water.
(16) Mosmann, T. (1983) Rapid colorimetric assay for cellular growth and survival: application to proliferation and cytotoxicity assays. *J. Immunol. Methods 65*, 55−63.
(17) Liu, Z., Li, Y., Lozada, J., Schaffer, P., Adam, M. J., Ruth, T. J., and Perrin, D. M. (2013) Stoichiometric leverage: rapid 18F-aryltrifluoroborate radiosynthesis at high specific activity for click conjugation. *Angew. Chem., Int. Ed. 52*, 2303−2307.
(18) Mu, L., Höhne, A., Schubiger, P. A., Ametamey, S. M., Graham, K., Cyr, J. E., Dinkelborg, L., Stellfeld, T., Srinivasan, A., Voigtmann, U., and Klar, U. (2008) Silicon-based building blocks for one-step 18F-radiolabeling of peptides for PET imaging. *Angew. Chem., Int. Ed. 47*, 4922−4925.
(19) D'Souza, C. A., McBride, W. J., Sharkey, R. M., Todaro, L. J., and Goldenberg, D. M. (2011) High-yielding aqueous 18F-labeling of peptides via Al18F chelation. *Bioconjugate Chem. 22*, 1793−1803.
(20) Schirrmacher, R., Bradtmöller, G., Schirrmacher, E., Thews, O., Tillmanns, J., Siessmeier, T., Buchholz, H. G., Bartenstein, P., Wängler, B., Niemeyer, C. M., and Jurkschat, K. (2006) ^{18}F-labeling of peptides by means of an organosilicon-based fluoride acceptor. *Angew. Chem., Int. Ed. 45*, 6047−6050.
(21) Matsui, S., and Aidi, H. (1978) Hydrolysis of some N-alkylmaleimides. *J. Chem. Soc., Perkin Trans. 2*, 1277−1280.
(22) Radiochemical titration of the maleimide-AuNP **7** was carried out using [^{18}F]-SiFA-SH ([^{18}F]**5**). The Michael addition titration results indicate that >20% of the intact maleimide groups are present after controlled hydrolysis (leaving at least 6 intact maleimide group per **7**). Further titration with [^{18}F]**5**, however, leads to an insoluble product due to the high lipophilicity of the SiFA compounds.
(23) ^{1}H NMR spectroscopy with a model compound Br-TEG-tetrahydro-phthalimide. As shown in Figure S3, after reaction at 95 °C, pH 7 for 20 h, 35% of the maleimide moieties remain intact while 65% are hydrolyzed.